IEEE Transactions on Nuclear Science, Vol. NS-28, No. 3, June 1981

A NOVEL CURRENT MONITOR FOR DC AND MODULATED MAGNETS IN THE PROTON STORAGE RING*

B. R. Sandberg
Los Alamos National Laboratory, Los Alamos, NM 87545

The zero flux dc current transformer has been described before in literature.[1-2] This paper endeavors to present a more analytical approach. The method of demodulating the dc channel is novel, using a time-domain scheme rather than the usual second-harmonic method. The current monitor measures bipolar currents up to 2 000 A without physical contact of the single-turn primary. Choosing the secondary current as 1 A sets the turns ratio at 1:2000. The magnetic material used is of the molybdenum Permaloy variety with its high (30 000) initial permeability and almost square hysteresis loop. Its saturation flux density is about 0.74 T. The toroidal geometry of the tape-wound transformer insures almost unity coupling of the windings.

As depicted in Fig. 1, the ac channel consists of one toroidal transformer with bifilar wound secondaries. R_2 and the input impedance of the differential input amplifier must be very large; otherwise they would rob ampere-turns from N_2I_f, and a serious error would appear in the output voltage across R_0. As seen in the figure, the ac channel has a 3-db bandwidth from a low-frequency pole to infinity. The amplifier extends the transformer output response to lower frequencies by a factor of almost A_F; and the mutual inductance of the windings takes over at higher frequencies above the bandwidth of the amplifier.

At frequencies above ~ 500 kHz the resonances in the transformer's secondary windings become active and a simple low pass R-C filter could be used to eliminate them. The output voltage across R_0 is not within the feedback network. Therefore R_0 must be a very high-quality resistor in terms of temperature stability and accuracy.

Figure 2 shows a dc channel. Two toroidal transformers are used that are identical to the one employed in the ac channel. This circuit is obviously a sampled data or discrete system. The state of the net error current, $I_E = (N_1/N_2)I_1 - I_f$, is determined every period, T_s, of the square wave switching voltage V_{DR}. If the net error current I_E is not zero, a correction is made by I_f to bring it toward zero. I_f also flows through R_0 producing an output voltage, V_0, proportional to the input current I_1.

The best way to understand this dc channel is to study the actual waveforms in Fig. 2 that are shown for two conditions: with $I_E = 0$ and with $I_E > 0$. I_1 is greater than zero in both cases and steady. The toroids, flux biased by I_E, are both switched by V_{DR} from one saturated state to the other in such a way that, except for a very short interval proportional to I_E, no net voltage is induced in the primary or the secondary windings in series with R_0. Thus the secondaries in series present only $2R_c$ as a load to the power amplifier Vp. The toroids must be selected and matched by their switching time under a constant voltage low-impedance source. The signal derived from R_{DR} in series with the switching windings is squared up by an adjustable dead zone and limiter circuit.[3] The purpose of this adjustment is to zero the output voltage with $I_1 = 0$. Note the finite slope of the signal across R_{DR} as the toroids go into saturation.

The voltage switching signal V_{DR} and the demodulator signal V_{DS} must be in synchronism and are derived from a two-stage Johnson counter. These unipolar, logic level signals are level shifted by nonsaturating, differential input amplifiers to provide the 11.5-V bipolar signals that feed the dead-zone and limiter circuits. The actual demodulator is a simple summing amplifier circuit that adds and inverts the demodulating signal and the squared signal across R_{DR} followed by another dead-zone and limiter circuit. Thus the demodulator provides a bipolar, impulse-like signal of strength V_DT_0 when $I_E = 0$. T_0 is made short by adjusting the frequency $1/T_s$ of the clock that drives the Johnson counter so that the toroids saturate, with $I_E = 0$, about 50 µs before $T_s/4$.

*Work performed under the auspices of U.S. Department of Energy.

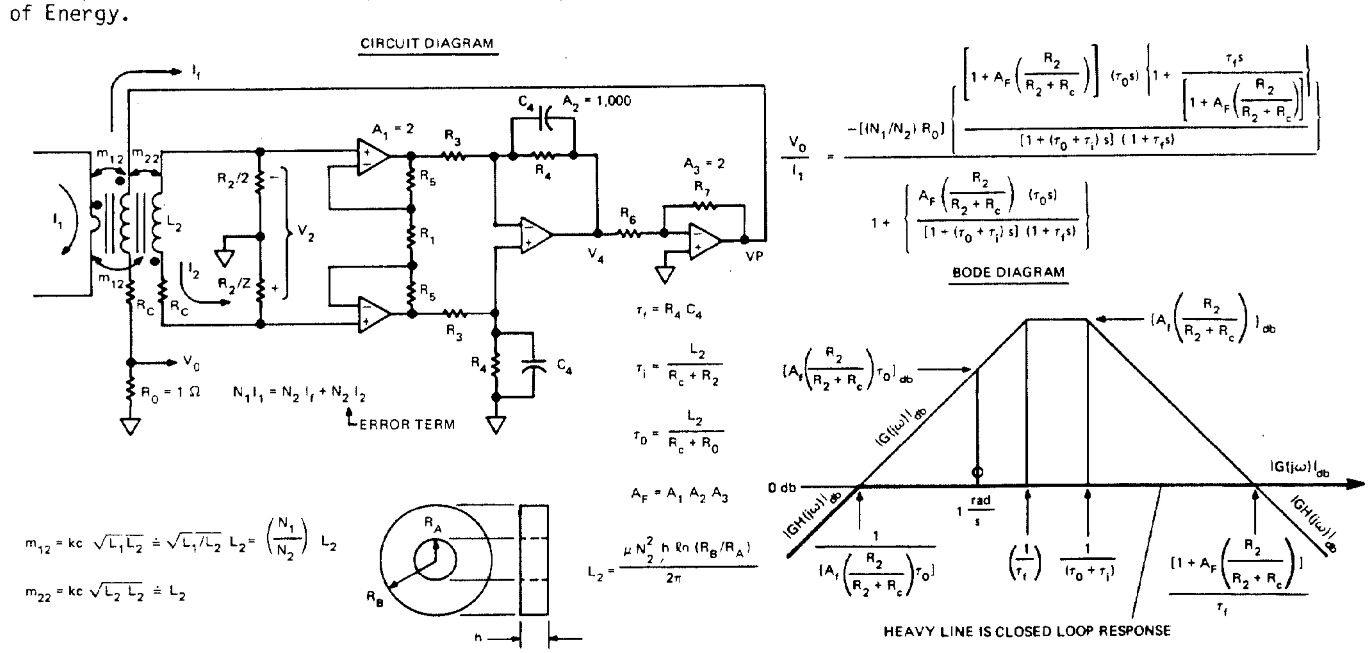

Fig. 1.

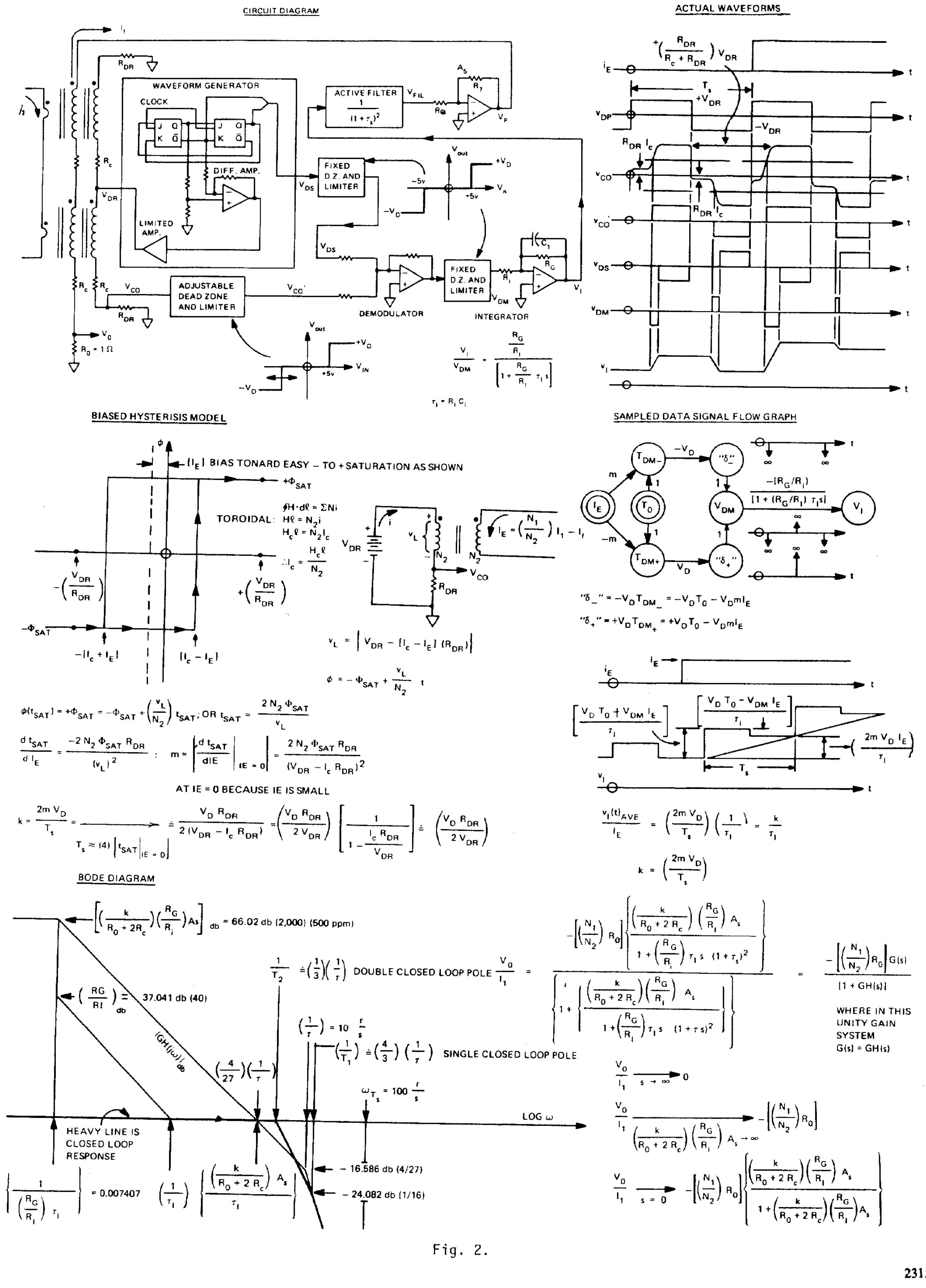
CIRCUIT DIAGRAM
WAVEFORM GENERATOR
CLOCK
DIFF. AMP.
LIMITED AMP.
ACTIVE FILTER
FIXED D.Z. AND LIMITER
ADJUSTABLE DEAD ZONE AND LIMITER
DEMODULATOR
INTEGRATOR
ACTUAL WAVEFORMS
BIASED HYSTERISIS MODEL
BIAS TONARD EASY – TO + SATURATION AS SHOWN
TOROIDAL:
AT IE = 0 BECAUSE IE IS SMALL
SAMPLED DATA SIGNAL FLOW GRAPH
BODE DIAGRAM
= 66.02 db (2,000) (500 ppm)
37.041 db (40)
DOUBLE CLOSED LOOP POLE
SINGLE CLOSED LOOP POLE
LOG ω
HEAVY LINE IS CLOSED LOOP RESPONSE
= 0.007407
– 16.586 db (4/27)
– 24.082 db (1/16)
WHERE IN THIS UNITY GAIN SYSTEM G(s) = GH(s)

Fig. 2.

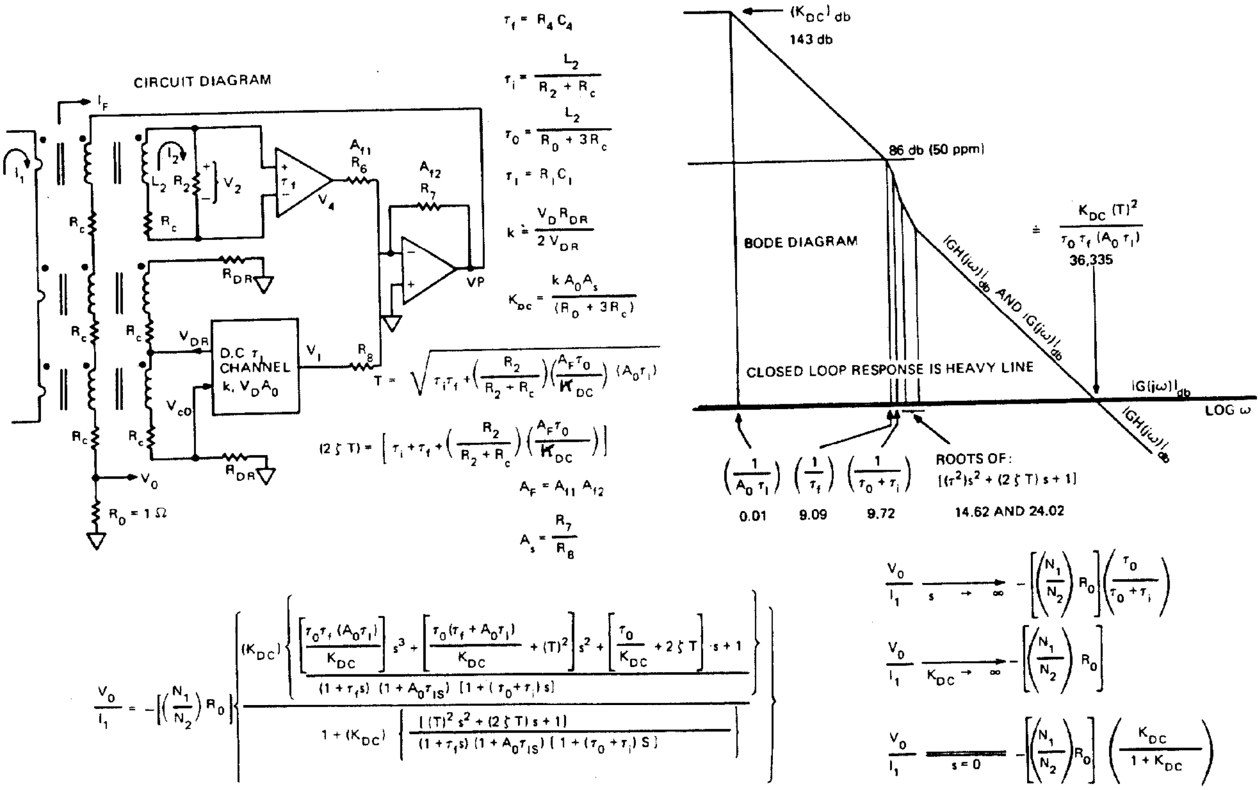

Fig. 3.

The integrator following the demodulator is purposely degraded by R_G to lower the open loop gain. However like all op-amp integrators it displays a constant gain, R_G/R_I, below the radian frequency $1/(R_G/R_I)(R_IC_I)$. The integrator converts the bipolar "impulses" from the demodulator to a "square" wave of voltage riding on a dc level proportional to the input current I_1. The following active low-pass filter allows this dc level to proceed through the dc channel, eventually determining the current I_f that flows through R_0.

Figure 2 also shows a signal flow graph of the sampled data portion of the dc channel. I_E and T_0 are inputs to this graph with V_I the integrator output. The biasing effect of I_E on the switching time of the toroids is indicated by m (sA^{-1}). V_D is the limiting voltage of the demodulator. The figure also shows the idealized time domain output of the integrator with a step of I_E applied. From this diagram it is easy to characterize the sampled data portion of the dc channel with a single parameter k(Ω) for all frequencies, an octave or lower, below the switching frequency $1/T_S$.

It remains to relate m and k to other circuit parameters. For this a simple flux-biased hysteresis model is used and shown in Fig. 2. The significant approximation here is that T_S is four times the toroid saturation time t_S with $I_E = 0$. This is justified because I_E is the net error current and therefore very small. The Bode plot is shown in Fig. 2. Using the criterion of no ringing in the output of this third-order system, the gain K_{DC} is adjusted so that two of the closed loop poles merge on the negative real axis.

To have current monitor with 50-ppm resolution at dc and still have a wide bandwidth, the ac and dc channels must be combined. The ac channel described above would continually drift toward flux saturation because of small offsets in its channel. The dc channel has short-interval large-amplitude switching spikes proportional to I_E in its output signal. A combination of the two channels eliminates both these catastrophes. The ac channel detects the spikes as an error signal and also serves as the active filter. The dc channel senses the drift as an error signal. Thus the two channels combined are a perfect marriage.

Figure 3 shows a summing amplifier as the method of combination. There are now three toroids. A standard, nondegraded integrator is used to achieve maximum open loop gain at dc. All of the design criterion of the individual channels remain in effect. The system transfer function is indicated along with Bode plot. Several different Bode plots are possible with this system, but large open loop gain at dc, large R_2, and no ringing in the output lead to the one shown.

In conclusion, a very accurate wide-band current monitor is achieved by the combination of an ac and a dc channel with toroidal transformers. The ac channel and transformers handle the fast components of the input current while the dc channel eliminates the drift and yields a precise reading at dc.

References

1. K. Unser, "Beam Current Transformer with dc to 200-MHz Range," IEEE Trans. Nucl. Sci., NS-16, 9340938.
2. M Groenenboom and J. Lisser, "Accurate Measurement of dc and ac by Transformer," Electonics and Power, January 1977, 52-55.
3. J. Smith, "Modern Operational Circuit Design," Wiley-Interscience, 1971.